Experimental Brain Research (2019) 237:687–703
https://doi.org/10.1007/s00221-018-5451-8

RESEARCH ARTICLE

Variable and intermittent grip force control in response to differing load force dynamics

Francis M. Grover[1] · Patrick Nalepka[2] · Paula L. Silva[1] · Tamara Lorenz[1,3,4] · Michael A. Riley[1]

Received: 19 July 2018 / Accepted: 6 December 2018 / Published online: 12 December 2018

Abstract

A recent study (Grover et al. Exp Brain Res 236(10):2531–2544, 2018) found that the grip force applied to maintain grasp of a hand-held object exhibited intermittent coupling to the changing load forces exerted by the object as it was oscillated. In particular, the strength and consistency of grip force response to load force oscillations was tied to overall load force levels and the prominence of load force oscillations. This contrasts with previous reports of grip force-load force coupling as generally continuous and stable and, therefore, has implications for theoretical accounts of grip force control that are predicated on these prior understandings of the coupling. The finding of intermittency additionally raises questions about the consistency of the temporal relation (i.e., lead/lag) between grip force and load force over time. The objective of the current study was, therefore, to investigate how the time-varying pattern (i.e., the regularity vs. complexity) of load force variations contribute to shifts between more intermittent and more continuous grip force control, and to determine the temporal consistency of the coupling. It was found that grip force became more tightly and continuously responsive to load force as load force changes became less predictable. Additionally, we report strong evidence that the temporal (i.e., lead/lag) relation between grip force and load force and the strength of their coupling vary substantially over time.

Keywords Grip force-load force coupling · Intermittency · Predictability · Recurrence quantification analysis

Introduction

Grip force (GF)–load force (LF) coupling refers to the ability to modulate grip in response to the changing LF exerted by an object as it is grasped and moved. Humans are remarkably adept at maintaining control of hand-held objects while wielding them, indicating a robust ability to tune GF adjustments in anticipation of LF changes. GF–LF coupling is typically characterized as a continuous and stable behavior (Flanagan et al. 1993; Flanagan and Wing 1993, 1995, 1997; Johansson and Westling 1984, 1987; Wing and Lederman 1998), with GF adjustments described as roughly in-phase with LF changes (e.g., Blank et al. 2001; Flanagan and Tresilian 1994; Viviani and Lacquaniti 2015). Additionally, GF adjustments reportedly occur with as little as a 10–15 ms lead or lag relative to LF changes (Flanagan and Wing 1995).

In a recent study (Grover et al. 2018), however, we found evidence for intermittency (i.e., irregular phasing between no or weak and strong coupling) in GF–LF coupling during 30 s bouts of oscillations of a hand-held object. As LF oscillated, GF was not continuously synchronized with LF but instead was often consistently much greater than LF with occasional bouts of more synchronous GF modulations. Intermittency was especially apparent during conditions in which LF variations were less pronounced compared to conditions yielding more definite LF oscillations. Occasional switches between more intermittent and more continuous coupling also occurred within individual trials.

Grover et al. (2018) also showed that lead-lag relations as calculated from a single-cross correlation analysis of

✉ Francis M. Grover
groverfm@mail.uc.edu

[1] Department of Psychology, Center for Cognition, Action, and Perception, University of Cincinnati, Edwards Center 1, Cincinnati, OH 45221-0376, USA

[2] Department of Psychology, Centre for Elite Performance, Expertise and Training, Macquarie University, Sydney, NSW, Australia

[3] Department of Mechanical and Materials Engineering, University of Cincinnati, Cincinnati, OH, USA

[4] Department of Electrical Engineering and Computer Science, University of Cincinnati, Cincinnati, OH, USA

averaged movement cycles (cf. Viviani and Lacquaniti 2015) disagreed substantially with the same calculations computed over a full trial, suggesting that GF–LF coupling is not consistent over time. These findings raise issues for the analytic approaches conventionally used to study the temporal aspects of GF–LF coupling, which usually involve single-value (e.g., mean or maximum) indicators of coupling strength and lead-lag relations. These single-value indicators are usually calculated either by cross-correlation or cross-spectral analysis (Blakemore et al. 1998; Blank et al. 2001; Danion et al. 2007; Flanagan and Wing 1993), or by correlating key events (e.g., maxima or sudden slope increase) between GF and LF (Flanagan and Wing 1993; Flanagan and Tresilian 1994). These calculations are not sensitive to the possibility that the strength of coupling between GF and LF, or the temporal relation between the two, varies over time. Because the existence of time-varying structure in GF–LF coupling could be informative about the underlying control processes, this aspect of GF–LF coupling needs to be better characterized and understood.

The current study, therefore, aimed at expanding the findings of Grover et al. (2018) by further investigating the temporal stability of GF–LF coupling in response to manipulations of overall LF levels and of the time-varying pattern of LF variations. Two particular issues were the primary focus of this work: Qualitative shifts in modes of more intermittent or more continuous GF control, and the consistency of the temporal relation (i.e., lead/lag) between GF and LF over time.

LF magnitude vs. LF complexity

In Grover et al. (2018), the primary method used to manipulate LF oscillations—increasing movement frequency—affected overall LF levels as well as the dynamical nature of LF variations (i.e., the time-varying patterns of LF). This precluded the ability to identify any effects of LF dynamics on GF–LF coupling independent from the effects of LF magnitude (which was additionally manipulated in that study by varying object mass). However, Zatsiorsky et al. (2005) found differences in how GF was modulated in response to static (i.e., due to change in object mass) and dynamic (i.e., due to change in object accelerations) manipulations of LF. In particular, they observed that GF levels increased to a greater degree with static increases in LF than they increased with dynamic increases in LF. Thus, it is important to manipulate LF dynamics and overall LF levels separately to determine their independent (or potentially interactive) influences on GF–LF coupling. This was the primary goal of the present study, which sought to extend the findings of Zatsiorsky et al. by examining not only the dynamic versus static manipulations of LF, but also by utilizing conditions with qualitatively different LF dynamics.

In the current study LF dynamics were manipulated in the context of a tracking task presented in virtual reality (VR). Participants held a real object in their hand and tracked the movements of a virtual target viewed in VR. The virtual target moved in a highly regular (sinusoidal), stochastic (fBm, i.e., correlated random walk), or deterministic but chaotic fashion (i.e., the chaotic Lorenz system). This manipulation was employed to create conditions of varying movement—and thus LF—predictability and complexity. Changes in the dynamical nature of the movements of a target have been shown to differentially influence the control used to track it during isometric force production (Mazich et al. 2014; Pew 1974; Studenka and Newell 2013; Smithson 1997; Sosnoff et al. 2009; Stephen et al. 2008). The aim of the current study's investigation of LF dynamics was, therefore, to determine if GF control exhibited a qualitative shift as LF variations became less regular. In addition, in the present study different amounts of mass were added to the hand-held object as a second experimental manipulation to determine how the strength and stability of GF–LF coupling was influenced by greater overall LF levels.

Hypotheses

Two primary hypotheses (denoted by H and enumerated below) were motivated by the findings of our previous study focused on describing the dynamics of GF–LF coupling (Grover et al. 2018). First, we hypothesized that GF–LF coupling would exhibit intermittency, which would be indicated if periods of tight coupling would alternate irregularly with periods when GF was not tightly coupled to LF (H1). Second, we hypothesized that conditions in which LF variations would be diminished in magnitude would promote more intermittent GF–LF coupling, while conditions of greater magnitude of LF variations would promote more continuous and stable GF–LF coupling. Thus, specifically we expected that greater added mass would result in more continuous coordination (i.e., lower intermittency) between GF and LF (H2). It may not seem intuitive to predict that conditions of greater LF variation would yield more continuous and stable GF–LF coupling while lower GF variation would yield intermittent GF control. However, Grover et al. (2018, p 11) discussed how this type of control can arise in, and potentially enhance, many types of motor behaviors (cf. Loram et al. 2011). In particular, we expected that the control of GF is enhanced by reducing the computational/predictive burden placed upon the control system by only requiring active corrections when LF variations increase to a degree that threatens grasp. LF variations below this threshold would, therefore, be accounted for via intrinsic system

mechanics, such as viscoelastic properties of the musculoskeletal system that help stabilize movements independent of the CNS (termed "preflexes"; see Loeb 1995), as well as the interplay between sensorimotor noise and feedback delay. This has been termed the "drift-and-act" hypothesis (Milton 2013).

Our prior findings of intermittency additionally motivated a set of novel hypotheses for this study. We hypothesized that the temporal (i.e., lead/lag) relation between GF and LF would be variable within individual trials (H3). Because GF and LF have been observed to be intermittently coupled, the anticipatory nature of GF modulation is not expected to be constant over time. We also hypothesized that conditions in which LF variations were more regular and stable, and thus more predictable, would promote more intermittent GF–LF coupling, while conditions of more complex and unpredictable LF variations would promote more continuous and stable GF–LF coupling (H4). These latter hypotheses seem counterintuitive considering previous reports of GF control as continuous and proportional to LF (e.g., Johansson and Westling 1987). However, they are motivated by recent studies showing that GF is more responsive when sensorimotor uncertainty is greater (cf. Hadjiosif and Smith 2015; Gysin et al. 2008).

Method

Participants

Twenty-three undergraduate students (8 male, 15 female) from the University of Cincinnati participated in exchange for course credit. Their ages ranged from 18 to 23 years ($M \pm SD = 19.12 \pm 1.20$ years), height ranged from 149 to 196 cm (174.21 ± 12.31 cm), and weight ranged from 50 to 136 kg (82.24 ± 27.17 kg). Participants had a mean arm length of 62.0 cm (± 5.54 cm). All participants were self-reportedly right-handed and free of any neurological, motor, or balance disorders or recent injuries. Participants provided written consent prior to completing the study, and all study procedures and methods were reviewed and approved by the University of Cincinnati Institutional Review Board.

Materials and apparatus

Participants grasped a custom-designed, 3-D printed, plastic cylindrical object in the right hand between the thumb and forefinger (see Fig. 1a). All participants wore a golf glove with leather fingertips to control for the coefficient of friction between the object and grasping digits. The object had a base mass of 52.7 g (including the Polhemus sensor) and was designed to have symmetrical distributions of mass along each axis of rotation. Two plastic pegs extended orthogonally from the central cylinder in each direction, and ring weights could be attached to each of the pegs to permit manipulations of object mass. Two added mass conditions were used, 60 and 120 g (with 30 g ring weights attached to each peg, respectively, in sets of two and four).

Participants wore an Oculus Rift CV1 virtual reality (VR) headset, which displayed an immersive, 3-D virtual environment created using the Unity (v. 5.6.12, Unity Technologies, San Francisco, CA) game engine. Accelerometers in the headset and external position trackers were used to register participants' head movements to allow for dynamic visual interaction with the VR scene.

Object motions were tracked using a Polhemus Liberty magnetic motion capture system (Polhemus Corp., Colchester, VT). A Polhemus sensor was attached to the front end of the object's central disc (Fig. 1a). Object motions were registered by this system and communicated to Unity to control the dynamic position of the object's virtual

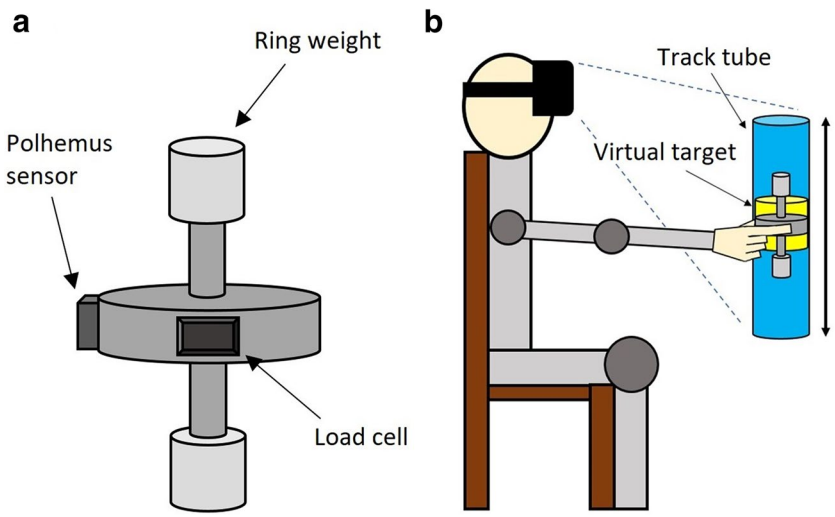

Fig. 1 **a** Weighted object design with locations of the load cell, Polhemus sensor, and ring weight application. **b** Movement task. Participants grasped the object and moved it vertically to coordinate with a moving virtual target shaped as a yellow cylinder. The target's range of motion was constrained by a longer, blue cylinder, which would flash to red when the virtual object's center was not sufficiently aligned with that of the target

counterpart. GF was measured directly using a FS20 low-force compression load cell (Measurement Specialties, Inc., Dayton, OH) embedded in the side of the hand-held object under the thumb's contact point. GF and motion data were sampled synchronously at a rate of 50 Hz.

Procedure

Each participant was seated in a chair facing the experimenter while grasping the real weighted object (see Fig. 1a) with their right hand. They were equipped with a VR headset displaying a virtual rendering of the experimental room along with a virtual rendering of the object. After aligning the real object with the virtual object, participants were able to see the virtual object move in virtual space while actually moving the real object. In the following the real and virtual object will, therefore, be treated as one and referred to as the weighted object. Two cylinders were rendered in the virtual environment (Fig. 1b). A small yellow cylinder served as the virtual target on which participants had to maintain the weighted object. A longer, translucent cylinder extended above and below the virtual target and served as a track tube to indicate the range of motion of the virtual target and help the participant constrain the motion of the weighted object to the vertical plane. In sum, the participant's task was to keep the weighted object inside the virtual target, which moved along the length of the track tube. Participants were instructed to hold the weighted object in front of them until it was aligned inside the virtual target. They were then instructed to track the virtual target as it moved vertically along the track tube by keeping the weighted object aligned with it. Participants were also instructed to keep the weighted object in a vertical orientation (see Fig. 1). The displacement of the virtual target (and the length of the track tube within which the target travelled) was proportional to the length of each participant's arm such that participant movements did not exceed 30° of shoulder flexion–extension.

The color of the track tube provided real-time visual feedback regarding how well the participant kept the weighted object oriented appropriately inside the track tube and in sufficient coordination with the virtual target. The track tube was shown in blue while performance was successful, and in red when there was an error. Error was indicated when the distance between the weighted object and virtual target was greater than 1/6 of the object's length (i.e., 2.1 cm) or when the weighted object's tilt (along any axis) exceeded 10°.

Three virtual target movement conditions were used, with sample virtual target trajectories shown in Fig. 2. In the first condition, the target did not follow a predictable trajectory and was instead driven by smoothed fractional Brownian motion (fBm; i.e., a correlated random walk, artificially generated to have a Hurst exponent of 0.25; smoothing was conducted to slightly reduce noise to make the target easier to track; Fig. 2a). In the second condition, the target followed a deterministic but seemingly random and fundamentally unpredictable trajectory (i.e., the chaotic Lorenz system with parameter values $\rho = 28$, $\sigma = 10$, $\beta = 8/3$ and initial x, y, and z values varying per trial; Fig. 2b). Different fBm (i.e., each a new randomly generated signal) and Lorenz (i.e., different initial conditions) trajectories were used for each trial repetition in these two conditions. In the third condition, the target followed a regular, cyclical, and predictable trajectory (i.e., a sine wave with frequency of 0.43 Hz; Fig. 2c). The parameters of the target trajectories were selected to present trajectories with reasonable difficulty (i.e., moving neither too slowly nor too suddenly or erratically) and that minimized variation in basic LF levels and movement smoothness across trajectory conditions. Target trajectories were the same for all participants. Each trial lasted 30 s, and total experimentation time was 10.5 min. To avoid fatigue, each participant was given the option to rest (for as long as they liked) between every trial and then received a 5-min break between the different mass blocks. As a result, each experimental session lasted roughly 30 min.

Design

The two object mass conditions (60 and 120 g) along with three conditions of virtual target movement (sine, fBm, and Lorenz) resulted in a 3×2 within-subjects design. Three trials in each condition were performed, resulting in 18 total trials per participant. Conditions were blocked by mass and otherwise randomized.

Data processing and measures

Data processing

GF and motion data were first filtered using a 4th-order low-pass zero-lag Butterworth filter with a half-power frequency of 4 Hz. LF was defined as the linear sum of gravitational forces and inertial forces arising from object accelerations along the vertical axis. LF was derived from the object's positions via inverse dynamics calculations. Kinematic data were filtered at each step of differentiation (i.e., from position to velocity, and velocity to acceleration).

Assessment of basic task performance

Root mean square (RMS) deviation of the observed and Z score normalized object motions from the target motion trajectories was calculated for each trial to assess how well the participant coordinated with the target. Mean GF and LF levels as well as the variability (SD) of GF and LF were also calculated for each trial.

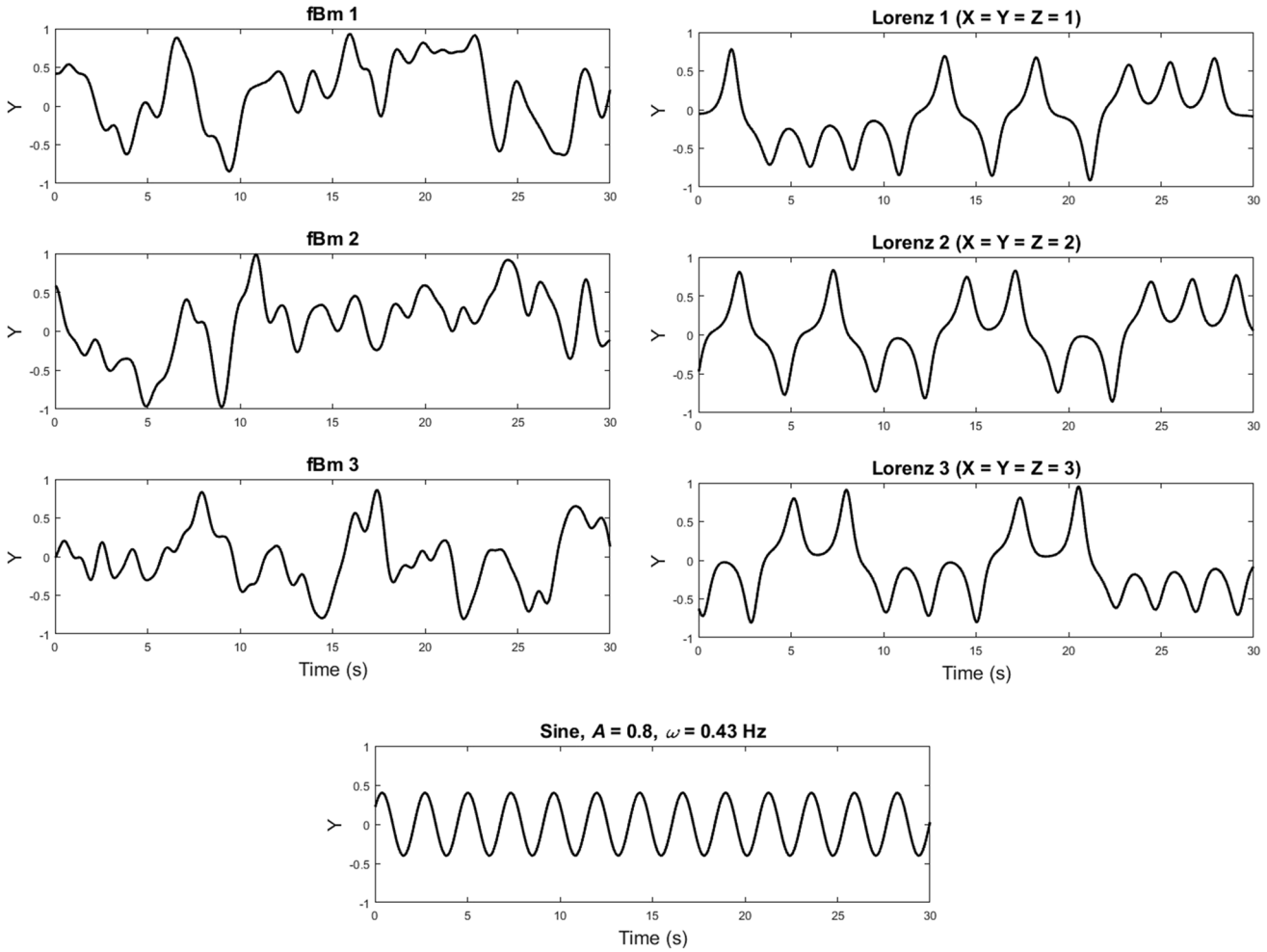

Fig. 2 Target trajectories. Initial conditions for the Lorenz trajectories are shown. *Y* axis units are in terms of position along the target track (i.e., 0 representing the center and ± 1 representing the upper and lower bounds)

Conventional assessment of coupling

Due to the aperiodic nature of the target movements in some conditions, dividing trials into cycles and averaging data across normalized cycles prior to measuring coupling using cross-correlation analysis (cf. Viviani and Lacquaniti 2015) was not possible. Therefore, cross-correlation measures of coupling were computed solely over the full trial. The time lag at which the maximum absolute cross-correlation coefficient occurred along with the magnitude of the coefficient at that time lag were obtained for each trial.

Windowed cross-correlation analysis

The specific objective of this analysis was to test the hypothesis (H3) that GF–LF coupling is time-varying against the null hypothesis that a continuously stable temporal relation exists between GF and LF. To accomplish this, a series of cross-correlations of the two time series (GF and LF) using a sliding window of a fixed number of samples was performed. Each window slid by one sample (thus overlap between windows was equal to window size minus one), and the cross-correlation function was inspected for change as the window moved through the time series. Greater change in the function over time was interpreted to indicate a temporally less stable coupling. Change in the cross-correlation function over time was quantified as variability (SD across all windows per trial) of the lags at which the two time series were maximally correlated within each window as well as the SD of the corresponding coefficient magnitudes. Trials with greater variability across cross-correlation windows were interpreted as having less stable GF–LF temporal relations.

Crucial to this analysis is choosing an appropriate window size: Too small a size would present too narrow a timescale per window for the cross-correlation to reliably reflect the signals' dynamics (which would result in an artificially inflated SD), while too large would present too wide a timescale per window to capture the potential variation

that is occurring over time (which would result in an artificially minimal SD). To facilitate this choice, the following method was used to determine a window size that would be appropriate for comparing signals with a known, stable relation. LF signals were compared to themselves at a fixed lag (25 samples, i.e., 0.5 s; Fig. 3a) to serve as a reference of a "coupling" with constant temporal relation. Given that this relation would show minimal variability in cross-correlations across windows, a window size was selected for each trial to minimize the variability that occurred across cross-correlation windows for these self-lagged LF signals. The smallest window at which the SD of the lags returned by cross-correlation windows fell below 0.01 s was selected for each trial. Then, window sizes were averaged across participants and trial repetitions to provide a window size for each condition (see Table 1) used to assess GF–LF coupling compared to LF-lagged LF coupling (Fig. 3b).

As each window shifted by one sample, each analysis consisted of n windows, equal to the total number of samples minus the window size (minus one) per trial. In addition to tracking the SD of the cross-correlation function for GF–LF coupling across experimental conditions, a scaling relation was plotted to examine how the SD of the cross-correlation function decreased as a function of window size, in comparison to the same function for self-lagged LF signals (Fig. 3b).

Cross-recurrence quantification analysis

The dynamics of GF–LF coupling were analyzed using cross-recurrence quantification analysis (CRQA; Marwan and Kurths 2002). CRQA quantifies how similarly two time series evolve over time in terms of how they visit common locations in a (reconstructed) phase space. Co-visitation appears as plotted recurrent "points," and consecutive points, i.e., "lines," indicate continuing recurrence. Using CRQA, the degree and stability of coordination between two time series can be quantified in a number of ways (Coco and Dale 2016).

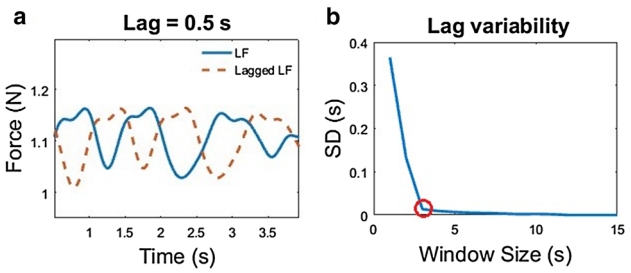

Fig. 3 **a** Example LF signal and a copy of it at a time lag of 0.5 s. For each trial, this served as a reference of a coupling with continuous temporal relation. **b** Window size for a particular condition was selected based on (an average of) the smallest window at which, for the compared LF signals, the SD of the lags returned by the sliding cross-correlation function fell below 0.01 s, as indicated by the red circle

Table 1 Window size for sliding cross-correlation

Trajectory	Mass	
	60 g	120 g
fBm	187 (3.74)	186 (3.72)
Lorenz	201 (4.02)	203 (4.06)
Sine	237 (4.74)	231 (4.62)

Window sizes are expressed in units of number of samples, with respective time (s) in parentheses

Out of the options provided by CRQA, based on previous findings (Grover et al. 2018) our analysis focused on its vertical line measures (Marwan et al. 2002). These measures quantify the relative degree of continuous versus intermittent coupling between two signals and were used to test H1, H2, and H4. The percentage of points which fall on vertical lines in a cross-recurrence plot indicates laminarity, the tendency for one signal (i.e., GF) to get "trapped" with respect to a single value of the other signal (i.e., LF), which is associated with intermittency in the coupling between two signals. The average vertical line length is referred to as trapping time, which reflects how long, on average, one signal remains (or gets "trapped") in a specific state of the second signal. Maximum vertical line length indicates the maximum amount of time that one signal is trapped by the other.

Preliminary analyses revealed the presence of nonstationarity within GF time series. When using a fixed neighborhood size (sometimes termed a fixed radius value), CRQA is vulnerable to miss instances of coordination occurring between two signals if one signal has drifted from the other. Therefore, a fixed-recurrence rate was employed, which used a flexible neighborhood size (Fig. 4). This method adaptively modulates the radius to ensure that a fixed number of recurrent points is identified (here, 5% of all possible comparisons; see Webber and Marwan 2015). Thus, it is able to register recurrences (and thus patterns of coordination) that would be dropped due to drift in one or both of the signals and is more robust than attempting to detrend GF signals that drift at different rates. While this eliminates recurrence rate as a measure that can be analyzed, it aids the reliability of the remaining CRQA measures, such as laminarity, trapping time, and vertical line length.

Values for the CRQA parameters delay and embedding dimension were determined using methods provided by Webber and Marwan (2015). Delay values were found to vary only slightly from trial to trial and ranged from 14 to 15 samples (280–300 ms) while an embedding dimension of 4 was indicated for every trial. Prior to phase space

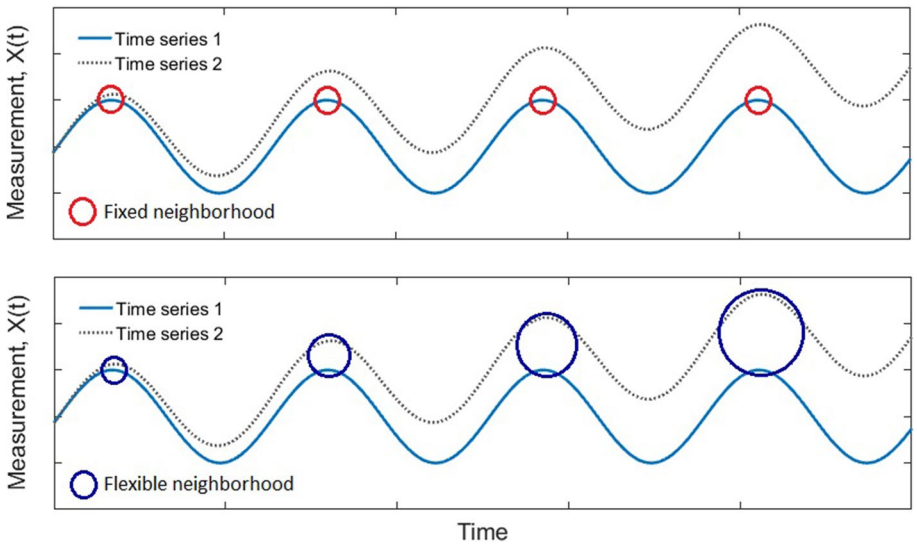

Fig. 4 Schematic of comparing recurrence between two time series when one exhibits nonstationarity in the form of drift. The blue circles illustrate how CRQA using a flexible neighborhood size is able to register co-visitation in reconstructed phase space in the face of drift that is not identified when using fixed neighborhoods (red circles)

reconstruction and CRQA calculations, the signals were rescaled by centering each about their respective medians.

Statistical analysis

After screening for outliers (median ± 2.5 SD), dependent variables were first averaged over repeated trials in the same condition for each participant. Those average values were then submitted to a separate (for each measure) 2 × 3 repeated-measures analysis of variance (ANOVA) to assess the effects of object mass and target trajectory. A Greenhouse-Geisser correction was applied to the degrees of freedom for the ANOVAs where the assumption of sphericity was violated. Simple-effects analyses and Bonferroni-corrected post-hoc tests were applied as needed to follow-up on significant effects.

Results

Basic task performance

The RMS deviation of participants' trajectories from the target trajectories (i.e., tracking error) revealed a clear pattern of coordination error decreasing significantly as added mass increased from 60 g (0.33 ± 0.07 SD) to 120 g (0.31 ± 0.07 SD), $F(1,21) = 18.47$, $p < 0.001$, $\eta_p^2 = .47$. Error also changed significantly across target trajectories, $F(1.42,29.76) = 133.60$, $p < 0.001$, $\eta_p^2 = 0.87$ (see Figs. 5, 6).

Error was greatest in the fBm movement condition (0.38 ± 0.05 SD), then decreased for the Lorenz condition (0.32 ± 0.05 SD, $p < 0.05$) and further for the sine condition (0.25 ± 0.05 SD, $p < 0.05$).

There was a significant effect of mass on mean LF, $F(1,21) = 1.97 \times 10^8$, $p < 0.001$, $\eta_p^2 = 1.00$. Mean LF increased from 1.11 N ($\pm 2.00 \times 10^{-4}$ N) in the 60 g condition to 1.69 N ($\pm 3.00 \times 10^{-4}$ N) in the 120 g condition. ANOVA also indicated that mean LF changed across target trajectory conditions, $F(1.55,32.47) = 9.72$, $p < 0.001$, $\eta_p^2 = 0.32$. However, while this difference was statistically significant, which may have resulted from miniscule between-subjects variance (MSE = 9.86×10^{-8}), the quantitative differences in the mean LF values across trajectory were not substantial. The immense effect size of mass, in comparison, suggests that the effect of gravity dominated mean LF values, rendering the average overall LF essentially equal across trajectory conditions. Thus, the intent to manipulate overall LF via added mass while controlling for it across target trajectory conditions was deemed successful despite the significant trajectory effect.

Like LF, mean GF levels also increased significantly as a function of mass, $F(1,21) = 13.91$, $p = 0.001$, $\eta_p^2 = 0.40$,

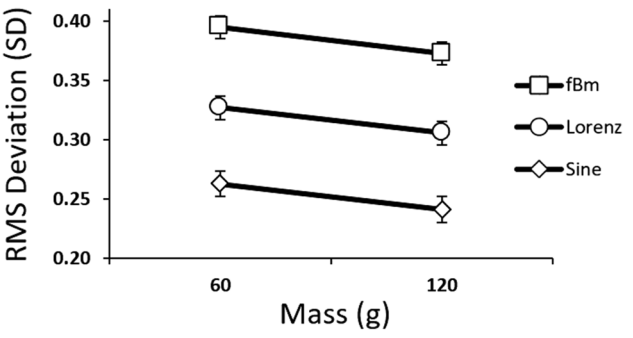

Fig. 5 RMS deviation of participant position from target position as a function of target trajectory and added mass. Error bars are ± 1 standard error of the mean

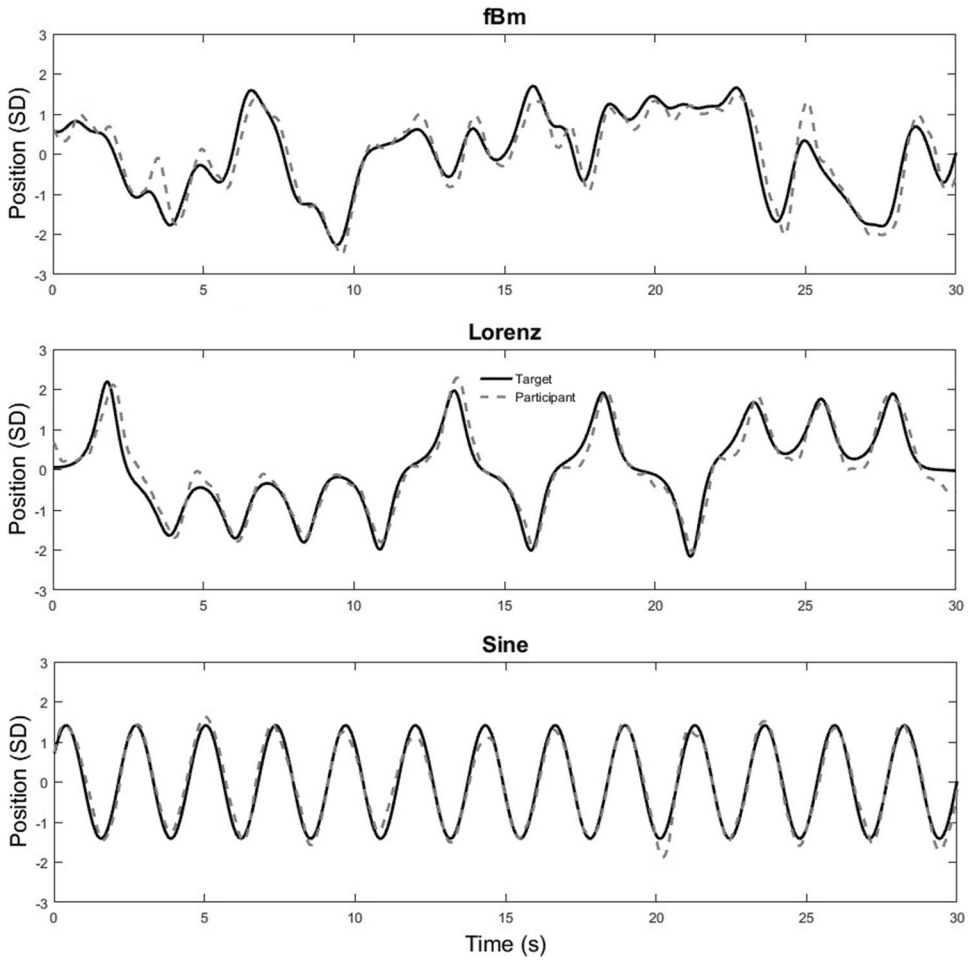

Fig. 6 Sample time series of participant motions superimposed on the target trajectories for each target condition in the 60 g added mass condition

increasing from 2.51 N (± 0.69 N) in the 60 g condition to 2.87 N (± 0.58 N) in the 120 g condition (see Table 2). However, mean GF was not significantly affected by target trajectory, $p > 0.8$.

The variability (SD) of LF increased significantly with added mass from 60 g (0.07 ± 0.02 N) to 120 g (0.10 ± 0.02 N), $F(1,21) = 224.68$, $p < 0.001$, $\eta_p^2 = 0.92$, as well as across target trajectories, $F(1.53,32.08) = 75.58$, $p < 0.001$, $\eta_p^2 = 0.78$. In particular, LF variability was significantly lower for the sine condition (0.07 ± 0.02 N) than the fBm condition (0.10 ± 0.02 N, $p < 0.001$) and the Lorenz condition (0.09 ± 0.02 N, $p < 0.001$). LF variability was also significantly greater for the fBm condition than the Lorenz condition, $p < 0.001$.

GF variability did not change significantly across trajectory ($p > 0.2$) or mass ($p > 0.1$) conditions.

Mean GF was positively correlated with GF variability, $r(134) = 0.41$, $p < 0.001$, as well as with LF variability, $r(134) = 0.26$, $p < 0.01$. GF variability was slightly positively correlated with LF variability, $r(134) = 0.18$, $p < 0.05$. No other correlations among the measures reported in this section were significant.

Analyses of coupling

Conventional assessments and qualitative characteristics of GF–LF coupling

The main effect of mass on mean GF indicated a proportional increase in mean GF to the amount of increase in mean LF, and the significant correlation between GF and LF SD confirmed a change in GF variability proportional to the change in LF variability. In addition, as added mass increased, and thus LF level and amplitude increased (Fig. 7a, b), not only did the overall level of GF increase, but GF appeared to be modulated in a different manner. Under less demanding LF conditions, GF appeared less responsive to LF variation (Fig. 7a), while in more demanding LF conditions GF modulations in response to LF variations were more salient (Fig. 7b).

Lead-lag relations derived from cross-correlation analyses indicated that GF typically led LF by, on average,

Table 2 Basic performance parameters

	Condition–trajectory, mass (g)											
	fBm, 60		fBm, 120		Lorenz, 60		Lorenz, 120		Sine, 60		Sine, 120	
	M	SD	M	SD	M	SD	M	SD	M	SD	M	SD
Mean (*N*)												
GF	2.53	0.74	2.75	0.53	2.45	0.74	2.90	0.63	2.46	0.61	2.92	0.56
LF	1.11	2e-4	1.69	4e-4	1.11	2e-4	1.69	4e-4	1.11	2e-4	1.69	3e-4
SD (*N*)												
GF	0.21	0.07	0.22	0.07	0.19	0.06	0.22	0.08	0.19	0.08	0.20	0.06
LF	0.08	0.01	0.12	0.02	0.07	0.01	0.11	0.02	0.06	0.01	0.08	0.01

All units are in Newtons (*N*)

M mean; *SD* standard deviation

almost 42 ms, with the lead ranging from around 0 to as much as 100 ms. However, ANOVA indicated no significant changes in this lead across conditions (all $p > 0.5$). Likewise, ANOVA performed on the Fisher's z-transformed cross-correlation coefficients revealed no significant effects (all $p > 0.5$).

Windowed cross-correlation analysis

Lead-lag relations calculated from windowed cross-correlation analysis designed to test H3 were found to have an average SD of 0.20 s, which was significantly greater than the average of 0.01 s found for the self-lagged LF signals at an equivalent window size (i.e., compared to this reference for what would be expected for perfectly stable coupling), $t(136) = 29.68$, $p < 0.001$, $d = 2.55$. The magnitudes

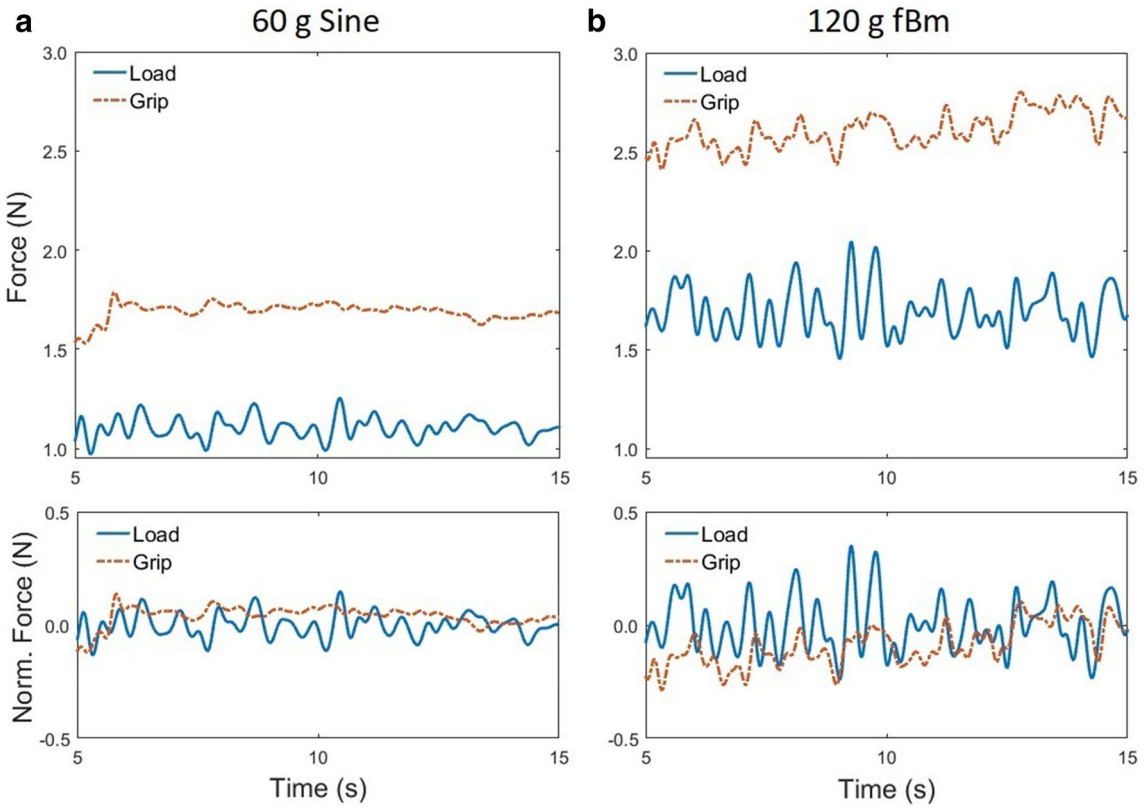

Fig. 7 GF and LF signals for mass conditions yielding minimum (**a**) and maximum (**b**) load amplitudes. Bottom plots show the signals after normalizing by centering each median around zero

of the Fisher's z transformed cross-correlation coefficients had an average SD of 0.14 s, which was also significantly greater than the reference value of 0.01 obtained from the self-lagged LF signals, $t(135) = 31.46$, $p < 0.001$, $d = 2.70$. Variability in the lead-lag relation and variability in coupling strength (indicated by the magnitude of the coefficient returned by cross-correlation windows) shared no significant linear relation, $r(134) = 0.06$, $p = 0.50$. ANOVA revealed no significant change in lead-lag variability or variability in coupling strength across conditions (all $p > 0.05$). These results support H3.

These findings are illustrated in Fig. 8, which depicts cross-correlation windows as a function of time. The uniform yellow band (yellow indicating strongest positive correlation) that is visible precisely at − 0.5 s lag for the self-lagged LF signals (Fig. 8, right) indicates the constancy of the "coupling" in that case; the two signals are maximally correlated at the same lag across all windows, reflecting how they were intentionally situated. As the left panel of Fig. 8 indicates, this was not the case for GF–LF coupling. The scattered patterns of yellow shading illustrate that the signals were maximally correlated at different lags and at different magnitudes (indicated by fainter or stronger shades of yellow) across windows (i.e., over time).

The scaling relation between window size and the variability in lags across windows did not exhibit the same pattern for GF–LF coupling as it did for self-lagged LF reference signals (Fig. 9). For all experimental conditions, the SD of the self-lagged LF signals rapidly decreased as window size increased and then remained at or around zero (Fig. 9, right). However, as the left panels in Fig. 9 illustrate, lead-lag SD for GF–LF coupling exhibited a much different trend, decreasing only slightly and rarely reaching a minimal value until the window size increased to almost the length of the full trial (at which point only a single cross-correlation is run, i.e., the SD is not defined). Additionally, plots of the mean and SD of this scaling relation for each condition revealed a large degree of variability across trials and participants for GF–LF, contrasting substantially with the minimal variability for respective self-lagged LF signals (Fig. 10), again in support of H3.

Cross-recurrence quantification analysis

CRQA was utilized to test the primary hypothesis (and corroborate the results from the windowed cross-correlation analysis) that GF–LF coupling exhibits a variable and potentially intermittent relation (H1), and to examine how the coupling changed across conditions (H2, H4). Cross-recurrence plots (CRPs) and their quantification supported H1 and, in support of H2 and H4, revealed a striking change in the nature of GF–LF coupling across conditions (Fig. 11), consistent with the visually distinct patterns apparent in Fig. 7. Trials in which GF modulations appeared least responsive to LF variations (Fig. 11b; left) yielded CRPs with longer and denser vertical line structures (Fig. 11a; left), indicating more intermittency in the coupling. In contrast, trials in which GF modulations appeared more strongly responsive to LF variations (Fig. 11b; right) yielded plots with less prominent vertical line structure (Fig. 11a; right) and more prominent diagonal line structure (i.e., more consistent coupling between LF and GF).

ANOVA revealed that laminarity decreased significantly as mass (and thus LF) increased, $F(1,21) = 29.43$, $p < 0.001$, $\eta_p^2 = 0.58$, in support of H2. Laminarity also changed significantly as a function of trajectory, $F(1.56,32.47) = 5.25$, $p < 0.05$, $\eta_p^2 = 0.20$, in support of H4. Laminarity was lowest in the fBm condition ($9.76 \pm 0.07 \times 10^{-1}$) and increased significantly from the fBm to the Lorenz condition ($9.79 \pm 0.05 \times 10^{-1}$), as well as from the fBm to the sine condition ($9.79 \pm 0.06 \times 10^{-1}$), both $p < 0.05$. The change in laminarity from sine to Lorenz was not significant, $p > 0.05$. As lower laminarity indicates less intermittency in the coupling, this indicates that coordination between GF and LF generally grew more continuous and less intermittent as mass increased. Additionally, coordination between GF and LF was generally more continuous and less intermittent in the fBm condition than in the sine or Lorenz conditions.

Trapping time followed a similar pattern, changing systematically as functions of both mass, $F(1,21) = 26.85$, $p < 0.001$, $\eta_p^2 = 0.56$, and trajectory, $F(1.72,36.09) = 6.24$, $p < 0.01$, $\eta_p^2 = 0.23$, respectively, supporting H2 and H4. Trapping time decreased from 60 g (7.52 ± 0.84 samples) to 120 g (6.84 ± 0.96 samples), indicating a decrease in the average amount of time that GF independently revisited specific LF states (i.e., became "trapped"). Like laminarity, trapping time was lowest in the fBm condition (6.89 ± 1.03 samples) and increased significantly from the fBm to the Lorenz condition (7.25 ± 0.91 samples), as well as from the fBm to the sine condition (7.43 ± 0.85 samples), both $p < 0.05$. The change in trapping time from sine to Lorenz (like laminarity) was not significant, $p > 0.05$.

Like laminarity and trapping time, maximum vertical line length (i.e., the maximum amount of time that GF was trapped by LF) changed significantly as a function of mass, $F(1,21) = 29.15$, $p < 0.001$, $\eta_p^2 = 0.58$, decreasing from 60 g (75.55 ± 14.35 samples) to 120 g (66.76 ± 12.17 samples) and providing support for H2. However, while maximum vertical line length changed significantly across trajectories, broadly in support of H4, $F(1.81,38.01) = 6.76$, $p < 0.01$, $\eta_p^2 = 0.24$, it changed in a

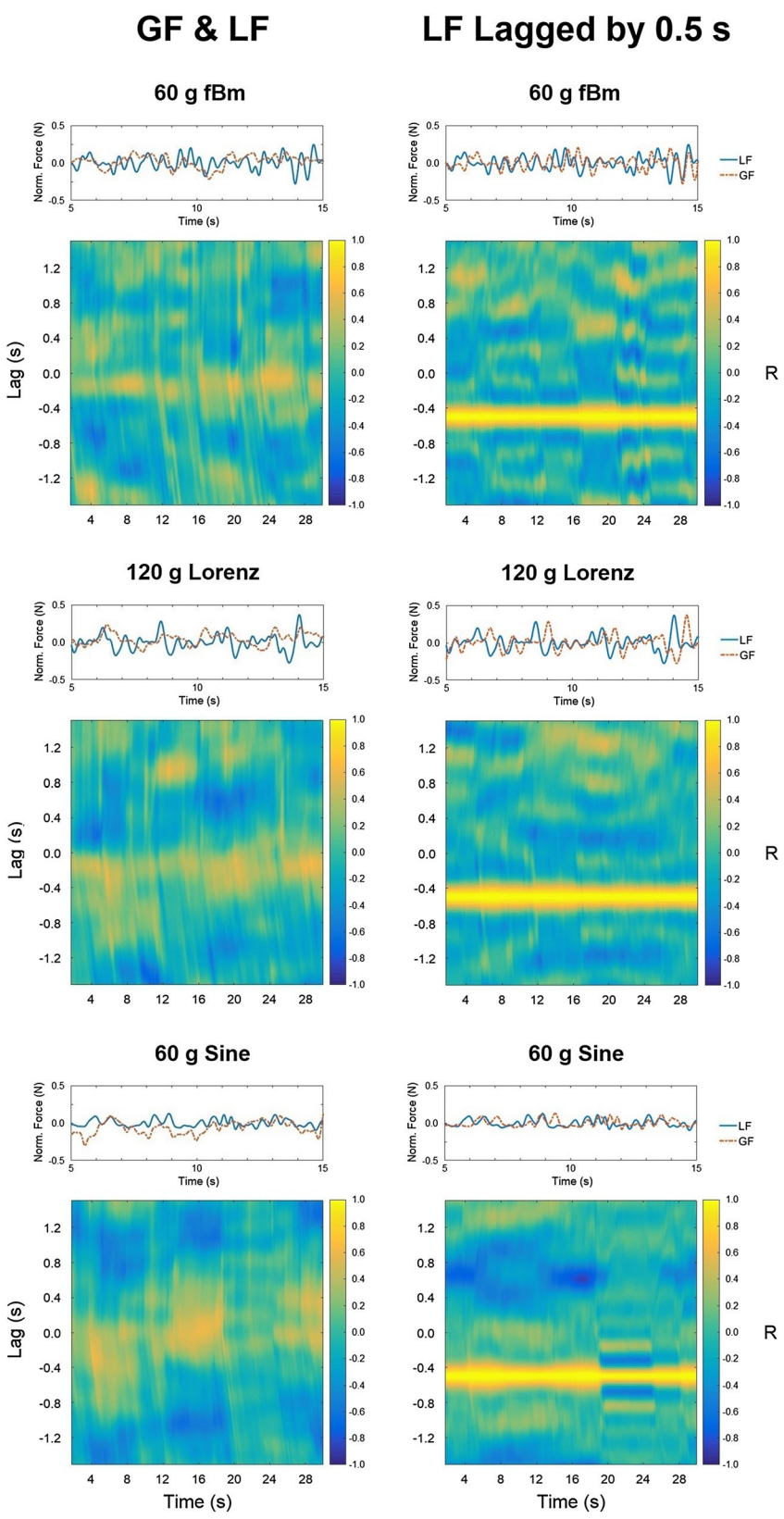

Fig. 8 Example trials displaying windowed cross-correlation as a function of time, comparing GF–LF coupling to the same function plotted for respective self-lagged LF signals. Each column in the plot represents the cross-correlation function for each window in time. The color shading indicates the coefficient magnitude increasing or decreasing as a function of lag (vertical axis). Thus, the consistency in coupling strength over time can be inspected by tracking the patterns of yellow shading horizontally across the figure

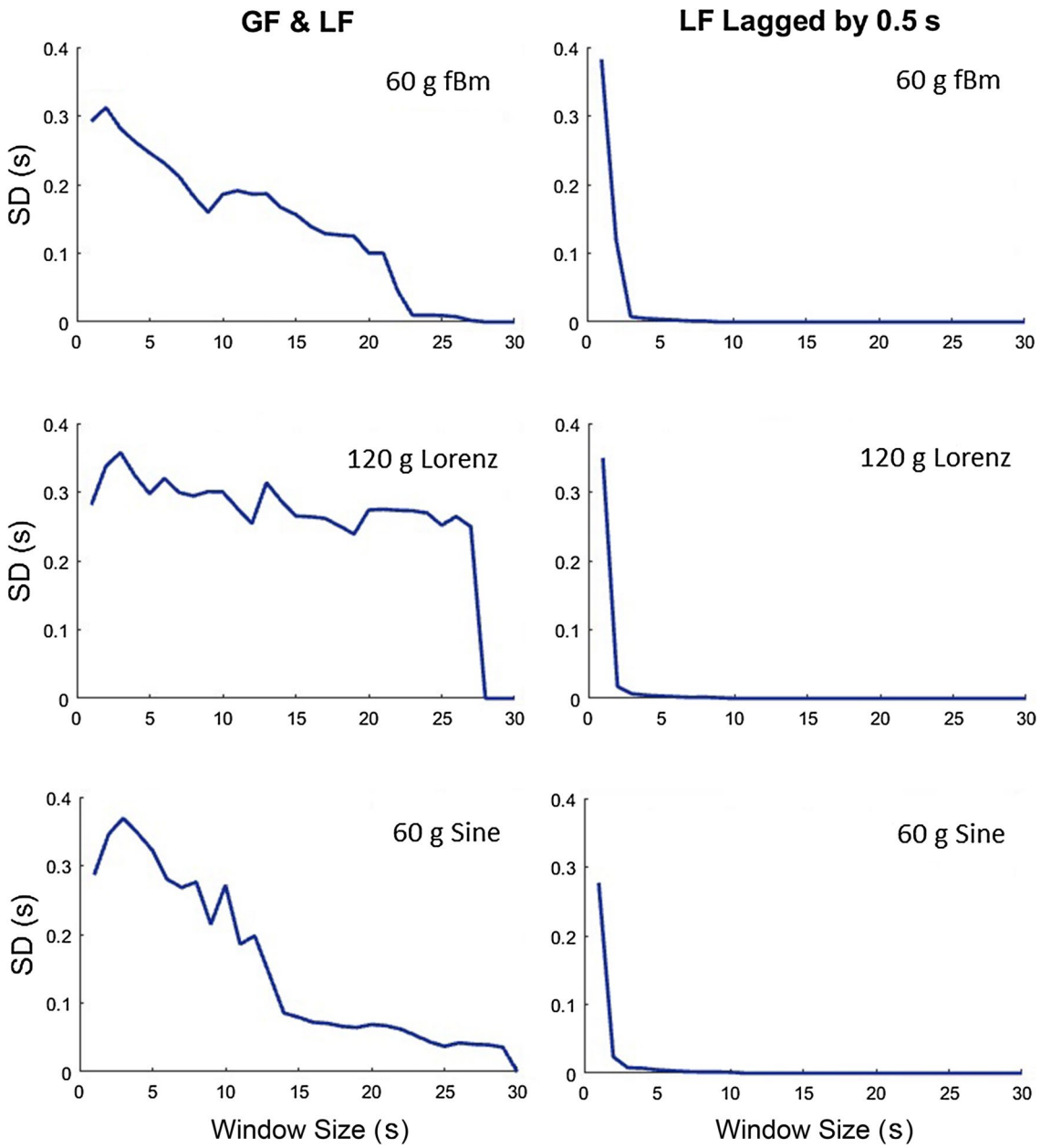

Fig. 9 For the same trials as Fig. 8, cross-correlation variability (SD) as a function of window size

contrasting pattern to that of laminarity and trapping time. Maximum vertical line length was greatest in the fBm condition (76.08 ± 17.68 samples) and decreased significantly ($p < 0.01$) from the fBm to the Lorenz condition (69.93 ± 11.61 samples) and from the fBm to the sine condition (67.53 ± 10.74 samples), $p < 0.01$ (Fig. 12). Like laminarity and trapping time, the difference between the sine and Lorenz conditions was not significant, $p > 0.05$.

Discussion

Intermittent and variable GF–LF coupling

The CRQA results replicated prior findings (Grover et al. in 2018)—intermittent responsiveness of GF–LF was again observed (supporting H1), particularly under conditions in which LF levels were lower (supporting H2). The results also supported our hypothesis (H4) that GF–LF coupling was more intermittent when LF was more regular and

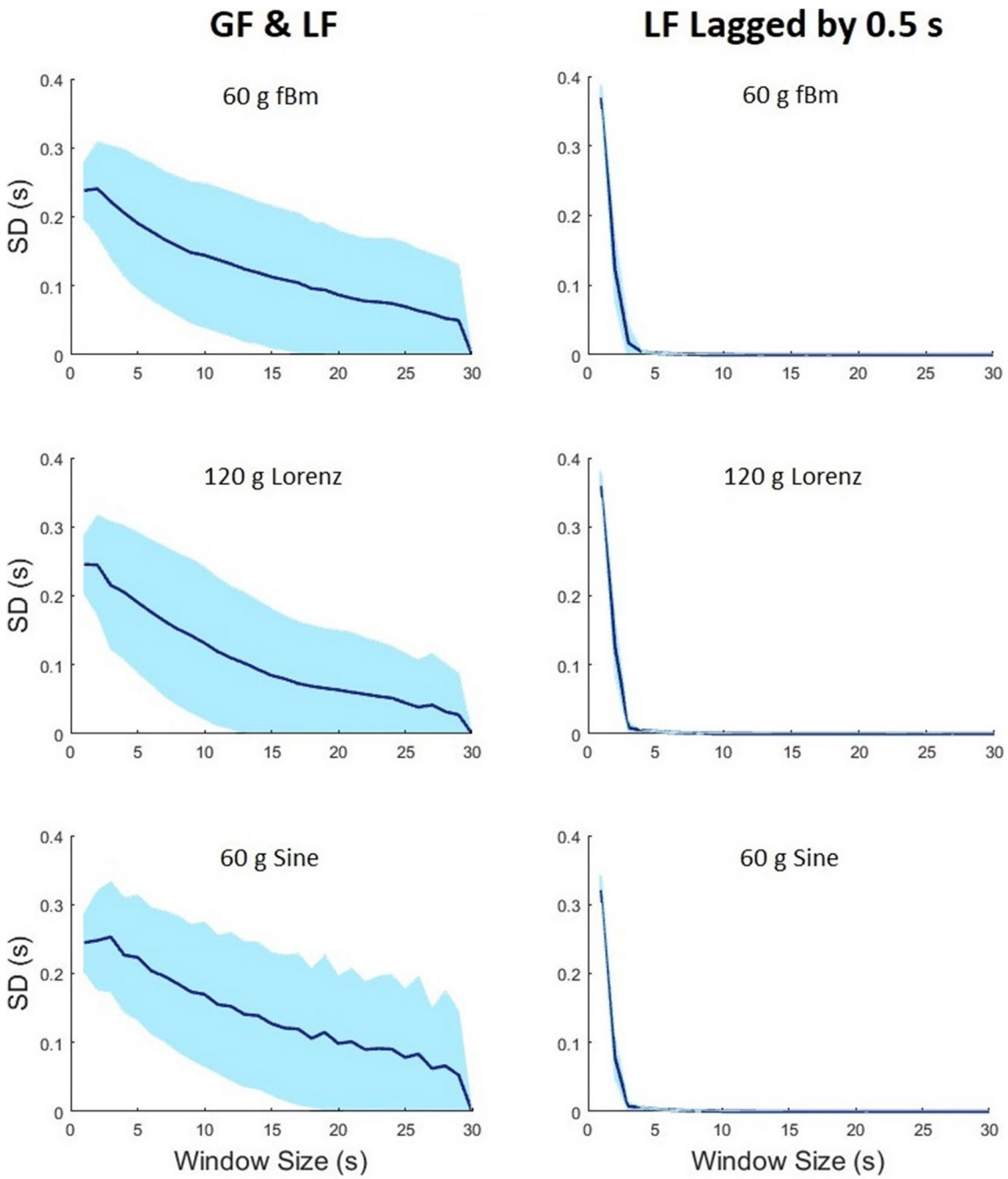

Fig. 10 The mean (line) and SD (shaded region) of cross-correlation variability (SD) as a function of window size (displayed for individual trials in Fig. 8) illustrating the scaling relation's distribution across trial repetitions and participants

predictable. As indicated by laminarity, the degree of intermittency in the coupling was greatest in the sine condition and lowest in the fBm condition.

The windowed cross-correlation results presented clear evidence that GF–LF coupling was not stable over the course of a trial, supporting H3. In particular, the variability of the lags at which GF–LF cross correlation was strongest and the variability of the magnitude of the correlation coefficient estimated at those lags, as illustrated in Fig. 10, were significantly larger than the corresponding variability evident in self-lagged LF signals exhibiting perfectly stable coupling. This presents strong evidence that GF–LF coupling is not as stable as typically construed (Blank et al. 2001; Flanagan et al. 1993; Flanagan and Wing 1993, 1995, 1997; Johansson and Westling 1984, 1987). Instead, both the temporal relation between

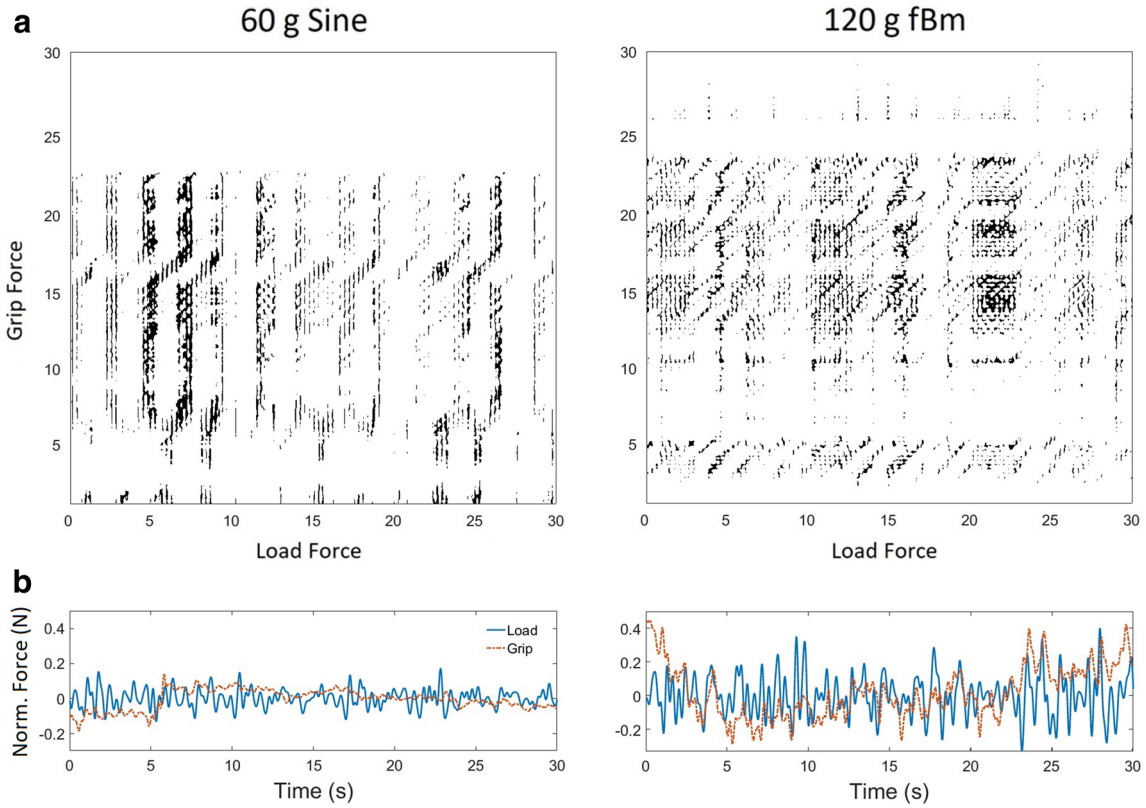

Fig. 11 **a** Cross-recurrence plots of LF vs GF. The axis units for the plots are in seconds, as each axis represents the respective signal's position over time in reconstructed phase space. **b** Normalized (centralized median) comparison of each force signal over time

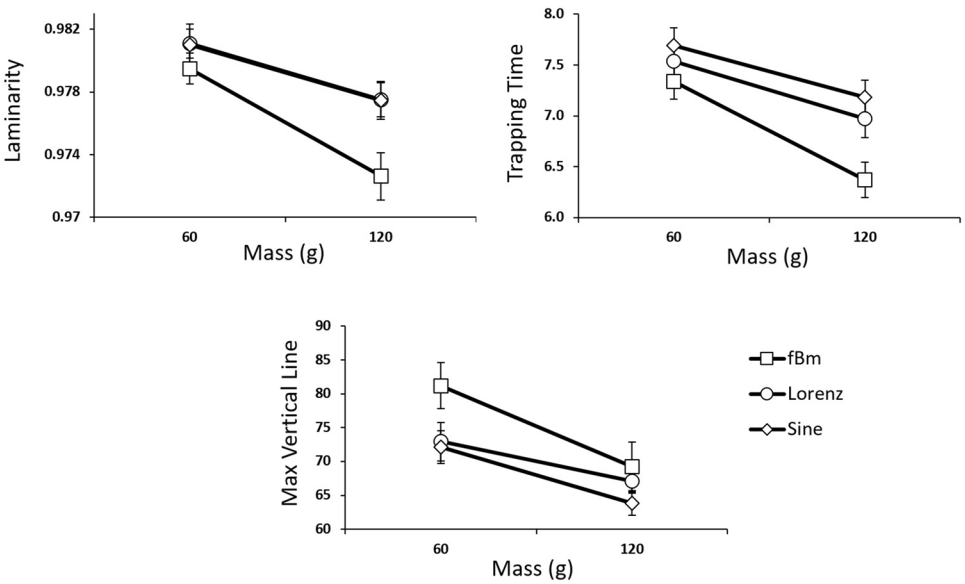

Fig. 12 Vertical line measures from CRQA as functions of target trajectory and mass. Interactions between mass and trajectory were not significant, all $p > 0.05$. Error bars are ± 1 standard error of the mean

GF and LF and the strength of their coupling appear to vary substantially over time.

The variability in the lags and coefficient magnitudes returned by the windowed GF–LF cross-correlation was not dependent on our choice of window size. As illustrated in Fig. 11, SDs only decreased gradually as window size increased, in contrast to what was found for the self-lagged LF signals, which dropped to near-zero values almost immediately after the initial smallest window size. This indicated that the variability in GF–LF coupling was

present regardless of how large the window was. Plots of the mean and SD of these scaling relations presented further evidence of inconsistent coupling in comparison to self-lagged LF signals. As Fig. 12 shows, the plotted scaling relation across window size for GF–LF coupling was also highly variable across participants, suggesting that the temporal stability of GF–LF coupling varies across individuals. For self-lagged LF signals, there was practically no variability across participants for any experimental condition.

Furthermore, the lack of a significant linear relation between variability of the lags and variability of the coefficient magnitudes showed that the two metrics were not artifacts of each other (i.e., the analysis did not automatically return a greater lag variability alongside greater coefficient variability). Therefore, variability in temporal relation and variability in coupling strength can be discussed, at least in the context of this study, as independent constructs.

These findings show that a single, full-trial cross-correlation analysis is not sufficient to accurately gauge the overall lead-lag relation or coupling strength (see also Grover et al. 2018). This claim is supported by the full trial cross-correlation results, which yielded lags (e.g., GF lead of up to 100 ms) and coefficient magnitudes (e.g., 0.14−0.15) that were inconsistent with prior findings (e.g., Flanagan and Wing 1995) and that did not change significantly across conditions, and hence did not capture what has typically been reported using this measure.

Additionally, these findings suggest that the emphasis on brief, discrete movement trajectories in most previous studies on GF–LF coupling does not lend itself to revealing how the dynamics of LF—especially complex LF dynamics, which are more representative of real world object manipulation—drive GF modulation. Similarly, most studies that examined cyclical, self-generated movements of hand-held objects either averaged their data across movement cycles or observed only a few (e.g., up to 4) movement cycles (Blank et al. 2001; Danion et al. 2007, 2009; Flanagan and Tresilian 1994; Flanagan et al. 1993; Flanagan and Wing 1995; Jaric et al. 2005; Viviani and Lacquaniti 2015), and thus have also not been able to capture how the relation between GF and LF might vary over time during longer bouts of behavior.

GF responses to changes in LF level and LF dynamics

The CRQA vertical line measures were greater when participants held the lighter than the heavier object (i.e., when LF variations were thus less salient), supporting H2, and across target trajectory conditions were lesser in the fBm condition when target movements (and thus LF variations) were least predictable, supporting H4. Together, these results suggest that perfect GF modulation is unnecessary under conditions when LF variations are either more subtle or more predictable, and as a consequence participants adopt an intermittent style of GF control. The support for H4 is consistent with findings by Gysin et al. (2008) and Hadjiosif and Smith (2015) that GF becomes more responsive as sensorimotor uncertainty increases. No significant interactive effects of manipulating LF level (i.e., object mass) and LF temporal dynamics (i.e., target trajectory) were observed, which is consistent with the reports of Zatsiorsky et al. (2005) regarding dissociable GF responses to static (i.e., object mass) and dynamic (i.e., changes in object accelerations) LF manipulations. The present results extend that work by showing that not only is GF modulated differently according to static and dynamic manipulations of LF level, but also is modulated differently when LF level is constant but the temporal pattern of LF variations changes in predictability.

GF–LF coupling in an implicit task setting

This study investigated GF–LF coupling in a task setting where the control of GF was not a salient task feature or explicit task goal for participants, but instead was implicit in completing a superordinate behavioral goal (tracking the target). The control of grasp or GF, per se, was not referenced in the instructions beyond telling the participants where to hold the object. This contrasts with many previous studies where GF control was a major task imperative for participants.

That the present results replicated the essential findings of intermittency from Grover et al. (2018) suggests that the implicit aspect of the task used in the present study did not seem to yield any substantial differences compared to explicit task settings used previously. However, given the differences in experimental procedures and in signal processing and analysis methods used in this study and Grover et al. compared to previous studies, it could still be the case that there are features of GF–LF coupling that could differ for tasks where GF control is a central focus made apparent to participants compared to tasks where GF control is not an obvious feature of the task (beyond not dropping a grasped object). It, therefore, remains important to directly compare instructions that manipulate GF control in a future study. Nevertheless, it may also be desirable for future studies of GF–LF coupling to utilize superordinate task goals (as used here, and is typically the case when holding objects in everyday life) whenever possible, both for the sake of increasing the ecological validity of laboratory studies and because it is ideal to limit subjects' ability to intuit researcher hypotheses so that there is less likelihood of demand characteristics or response bias.

Limitations and future directions

It was observed that coefficient magnitudes returned from the sliding window cross-correlation analysis were more likely to vary than the lag values even when the temporal relation of the coupling was stable. That is, even for self-lagged LF signals with an appropriate window size, the magnitude of the coefficients fluctuated slightly although the lag at which the maximum correlation coefficient was found remained constant. It is not clear whether this fluctuation in coefficient magnitudes simply requires a larger window size or whether it is the case that different dynamics will return slightly different cross-correlation functions, even given the same constant coupling. Thus, for signals that are not uniformly regular, no two windows will ever yield perfectly identical cross-correlation functions. This warrants further development of the windowed cross-correlation analysis to produce a metric that reliably but holistically captures the strength and temporal relation between GF and LF, and between coordinated subsystems in motor control more broadly.

The present findings suggest that GF–LF coupling may be a task-oriented phenomenon, that is, the modulation of GF may be organized in terms of the higher purpose of maintaining grasp of an object rather than simply automatically coordinating with LF changes. Thus, it could be useful in future studies to manipulate certain constraints pertaining to grasp that have not yet been investigated, such as the fragility of the object being grasped. It could additionally be useful to integrate the dynamics-focused methodologies of the current paper and Grover et al. (2018) with those constraints that have been studied, such as the coefficient of friction between the object and grasping digits (i.e., the object's "slipperiness"; Cole et al. 1999; Johansson and Cole 1992; Johansson and Westling 1984). The present findings suggest that GF adjustments would be sensitive to these constraints, and the degree of the stability of GF–LF coupling would likewise change in unique ways as the constraints are manipulated. Finally, a limitation of this study that would be useful to overcome in future studies is that we did not measure participants' grasp strength, and thus did not utilize LF conditions that required GF levels that were constant proportions of each participant's maximum voluntary contraction.

The variability of GF–LF coupling found in this study is consistent with recent research in the dynamics of chaotic oscillators which identified the potential for unidirectionally coupled systems (cf. Grover et al. 2018) to exhibit intermittent alternations among anticipatory, complete (i.e., no lag), and lagged coupling relations (Senthilkumar and Lakshmanan 2007). The pervasiveness of variability in GF–LF coupling over time suggests a need to investigate the potential for time-varying structure in the temporal relation between GF and LF and to explore whether a delay-differential equation modeling framework (see also Ambika and Amritkar 2009; Milton 2013; Stepp and Turvey 2009) can be fruitfully applied to capture the features of GF–LF coupling identified in this study and in previous studies.

References

Ambika G, Amritkar RE (2009) Anticipatory synchronization with variable time delay and reset. Phys Rev E Stat Nonlinear Soft Matter Phys 79(5):1–11. https://doi.org/10.1103/PhysRevE.79.056206

Blakemore SJ, Goodbody SJ, Wolpert DM (1998) Predicting the consequences of our own actions: the role of sensorimotor context estimation. J Neurosci 18(18):7511–7518

Blank R, Breitenbach A, Nitschke M, Heizer W, Letzgus S, Hermsdörfer J (2001) Human development of grip force modulation relating to cyclic movement-induced inertial loads. Exp Brain Res 138(2):193–199. https://doi.org/10.1007/s002210000622

Coco MI, Dale R (2016) Cross-recurrence quantification analysis of categorical and continuous time series: an R package. Front Psychol 5(355):1–31. https://doi.org/10.3389/fpsyg.2014.00510

Cole KJ, Rotella DL, Harper JG (1999) Mechanisms for age-related changes of fingertip forces during precision gripping and lifting in adults. J Neurosci 19(8):3238–3247

Danion F, Descoins M, Bootsma RJ (2007) Aging affects the predictive control of grip force during object manipulation. Exp Brain Res 180(1):123–137. https://doi.org/10.1007/s00221-006-0846-3

Danion F, Descoins M, Bootsma RJ (2009) When the fingers need to act faster than the arm: coordination between grip force and load force during oscillation of a hand-held object. Exp Brain Res 193(1):85–94. https://doi.org/10.1007/s00221-008-1597-0

Flanagan JR, Tresilian JR (1994) Grip-load force coupling: a general control strategy for transporting objects. J Exp Psychol Hum Percept Perform 20(5):944–957

Flanagan JR, Wing AM (1993) Modulation of grip force with load force during point-to-point arm movements. Exp Brain Res. https://doi.org/10.1007/BF00229662

Flanagan JR, Wing AM (1995) The stability of precision grip forces during cyclic arm movements with a hand-held load. Exp Brain Res 105(3):455–464. https://doi.org/10.1007/BF00233045

Flanagan JR, Wing AM (1997) The role of internal models in motion planning and control: evidence from grip force adjustments during movements of hand-held loads. J Neurosci 17(4):1519–1528. https://doi.org/10.1007/s00221-008-1691-3

Flanagan JR, Tresilian JR, Wing AM (1993) Coupling of grip force and load force during arm movements with grasped objects. Neurosci Lett 152(1):53–56. https://doi.org/10.1007/BF00229662

Flanagan JR, Bowman MC, Johansson RS (2006) Control strategies in object manipulation tasks. Curr Opin Neurobiol 16(6):650–659. https://doi.org/10.1016/j.conb.2006.10.005

Grover F, Lamb M, Bonnette S, Silva PL, Lorenz T, Riley MA (2018) Intermittent coupling between grip force and load force during oscillations of a hand-held object. Exp Brain Res 236(10):2531–2544. https://doi.org/10.1007/s00221-018-5315-2

Gysin P, Kaminski TR, Hass CJ, Grobet CE, Gordon AM (2008) Effects of gait variations on grip force coordination during object transport. J Neurophysiol 100(5):2477–2485. https://doi.org/10.1152/jn.90561.2008

Hadjiosif AM, Smith MA (2015) Flexible control of safety margins for action based on environmental variability. J Neurosci 35(24):9106–9121. https://doi.org/10.1523/JNEUROSCI.1883-14.2015

Jaric S, Russell EM, Collins JJ, Marwaha R (2005) Coordination of hand grip and load forces in uni- and bidirectional static force production tasks. Neurosci Lett 381(1–2):51–56. https://doi.org/10.1016/j.neulet.2005.01.086

Johansson RS, Cole KJ (1992) Sensory-motor coordination during grasping and manipulative actions. Curr Opin Neurobiol 2(6):815–823

Johansson RS, Westling G (1984) Roles of glabrous skin receptors and sensorimotor memory in automatic control of precision grip when lifting rougher or more slippery objects. Exp Brain Res 56(3):550–564. https://doi.org/10.1109/WHC.2013.6548481

Johansson RS, Westling G (1987) Signals in tactile afferents from the fingers eliciting adaptive motor responses during precision grip. Exp Brain Res 66(1):141–154. https://doi.org/10.1007/BF00236210

Loeb GE (1995) Control implications of musculoskeletal mechanics. Proceedings of the 17th international conference of the IEEE engineering in medicine and biology, IEEE, Montreal, Quebec, Canada, Canada, pp 1393–1394

Loram ID, Gollee H, Lakie M, Gawthrop PJ (2011) Human control of an inverted pendulum: Is continuous control necessary? Is intermittent control effective? Is intermittent control physiological? J Physiol 589(2):307–324. https://doi.org/10.1113/jphysiol.2010.194712

Marwan N, Kurths J (2002) Nonlinear analysis of bivariate data with cross recurrence plots. Phys Lett Sect A Gen Atomic Solid State Phys 302(5–6):299–307. https://doi.org/10.1016/S0375-9601(02)01170-2

Marwan N, Wessel N, Meyerfeldt U, Schirdewan A, Kurths J (2002) Recurrence-plot-based measures of complexity and their application to heart-rate-variability data. Phys Rev E Stat Nonlinear Soft Matter Phys 66(2):1–8. https://doi.org/10.1103/PhysRevE.66.026702

Mazich MM, Studenka BE, Newell KM (2014) Visual information about past, current and future properties of irregular target paths in isometric force tracking. Atten Percept Psychophys 77(1):329–339. https://doi.org/10.3758/s13414-014-0766-4

Milton JG (2013) Intermittent motor control: the "drift-and-act" hypothesis. In: Richardson MJ, Riley MA, Shockley K (eds) Progress in motor control. Springer, Berlin, pp 169–193. https://doi.org/10.1007/978-3-319-47313-0

Pew RW (1974) Levels of analysis in motor control. Brain Res 71(226):393–400

Senthilkumar DV, Lakshmanan M (2007) Delay time modulation induced oscillating synchronization and intermittent anticipatory/lag and complete synchronizations in time-delay nonlinear dynamical systems. Chaos. https://doi.org/10.1063/1.2437651

Smithson M (1997) Judgment under chaos. Organ Behav Hum Decis Process 69(1):59–66. https://doi.org/10.1006/obhd.1996.2672

Sosnoff JJ, Valantine AD, Newell KM (2009) The adaptive range of 1/f isometric force production. J Exp Psychol Hum Percept Perform 35(2):439–446. https://doi.org/10.1037/a0012731

Stephen DG, Stepp N, Dixon JA, Turvey MT (2008) Strong anticipation: sensitivity to long-range correlations in synchronization behavior. Phys A Stat Mech Appl 387(21):5271–5278. https://doi.org/10.1016/j.physa.2008.05.015

Stepp N, Turvey MT (2009) On strong anticipation. Cogn Syst Res 11(2):148–164

Studenka BE, Newell KM (2013) Visual information for prospective control of tracking irregular target paths with isometric force production. J Exp Psychol Hum Percept Perform 39(6):1557–1567. https://doi.org/10.1037/a0031744

Viviani P, Lacquaniti F (2015) Grip forces during fast point-to-point and continuous hand movements. Exp Brain Res 233(11):3201–3220. https://doi.org/10.1007/s00221-015-4388-4

Webber CL Jr., Marwan N (eds) (2015) Recurrence quantification analysis: theory and best practices. American Journal of Respiratory and Critical Care Medicine, vol. 168. Springer, New York. https://doi.org/10.1007/978-3-319-07155-8

Wing AM, Lederman SJ (1998) Anticipating load torques produced by voluntary movements. J Exp Psychol Hum Percept Perform 24(6):1571–1581. https://doi.org/10.1037/0096-1523.24.6.1571

Zatsiorsky VM, Gao F, Latash ML (2005) Motor control goes beyond physics: differential effects of gravity and inertia on finger forces during manipulation of hand-held objects. Exp Brain Res 162(3):300–308. https://doi.org/10.1007/s00221-004-2152-2